The racemization was expected to be much accelerated at elevated temperature,[22] but the chromium complex was found to decompose in hot solution. Hence, we could not clearly demonstrate if the equilibrium among the diastereomers also shifts in favor of *fac*-Λ in these cobalt(III) and chromium(III) complexes. However, the present study strongly suggests that noncovalent interligand interactions undoubtedly operate within a complex molecule, though its true depiction is not the right-handed (Figure 2) but the left-handed three-bladed propeller. In view of the above facts, we must retract a part of our previous conclusions on the cobalt(III) and chromium(III) complexes.[2,3,5]

It is seen from Table III that the CD induced at the ligand π–π^* transition is more intense in [M(*l*-moba-Me)$_3$] than in [M(*l*-moba)$_3$]. Hence, a higher stereoselectivity occurs in the *l*-moba-Me complexes, in agreement with the NMR spectral results for the Al and Ga complexes. This is probably due to a more efficient interaction in the *l*-menthyl/*p*-tolyl pair than in the *l*-menthyl/phenyl pair probably because of the increased π-electron density in the *p*-tolyl ring.[5,6] Table III further shows that the CD intensity increases on going from the Al to the In complex and from the Sc to the La complex in each ligand series. These facts imply that the CD intensity tends to increase when the central metal ion becomes larger, and this trend is more prominent when we adopt the asymmetry factor ($\Delta\epsilon/\epsilon$) instead of $\Delta\epsilon$, where the average is taken for the absolute values of two CD bands. When the $\Delta\epsilon/\epsilon$ values observed are plotted against the ionic radii (Shannon–Prewitt ionic radii[28]) of the metal ions, a good correlation is found between them, as shown in Figure 7. In this figure the data for [Gd(*l*-moba-Me)$_3$] determined in this study[29] are also included. The present result implies that efficient interligand *l*-menthyl/aryl interaction in [M(*l*-moba)$_3$] and [M(*l*-moba-Me)$_3$] becomes possible when the interacting groups can adopt a mutual orientation favorable for the interaction, and the ideal spatial matching of the interacting groups is attained when the central metal ion is considerably large ($r > 1.0$ Å). The above finding adds strong support to the noncovalent interligand interaction operating within complex molecules in the form of a left-handed three-bladed propeller.

This work was supported by Grant-in-Aid for Scientific Research No. 62430011 from the Ministry of Education of Japan. We are grateful to K. Ogi for NMR measurements and to H. Sakiyama for help in CD measurements.

(28) Shannon, R. D.; Prewitt, C. T. *Acta Crystallogr.* **1969**, *B25*, 925.
(29) Spectral data are as follows: AB, 336 nm (ϵ 40 500); CD, 351 nm ($\Delta\epsilon$ +12.3) and 318 nm ($\Delta\epsilon$ −8.8).

Contribution from the Department of Chemistry, The University of Texas, Austin, Texas 78712

Electrochemistry in Liquid Sulfur Dioxide. 8. Oxidation of Iron, Ruthenium, and Osmium Bipyridine Complexes at Ultramicroelectrodes at Very Positive Potentials

Edwin Garcia, Juhyoun Kwak, and Allen J. Bard*

Received April 12, 1988

The anodic potential range of liquid SO_2 for use in electrochemical studies was extended to about +4.7 V vs SCE by employing a new purification method and using tetra-*n*-butylammonium hexafluoroarsenate [(TBA)AsF_6] as supporting electrolyte. The anodic solvent limit occurs at potentials 0.7 V more positive than in previous studies and is attributed to supporting electrolyte oxidation. The electrochemistry of M(bpy)$_3^{2+}$ complexes (M = Fe, Ru, and Os) at −70 °C was studied by cyclic voltammetry at an ultramicroelectrode (25 μm diameter, Pt) with scan rates up to 10 kV/s. Fe and Ru oxidation waves to the 3+ form (metal-centered oxidation), and 4+, 5+, and 6+ species (bpy-centered oxidations) are observed. While the 4+ forms were stable, the 5+ and 6+ species decomposed, presumably by reaction with solvent or supporting electrolyte. For M = Os, waves for oxidation of stable, metal-center 3+ and 4+ species are observed. A third wave, to an unstable 5+ species, represented as $Os^{IV}(bpy^{\cdot+})(bpy)_2$, is also seen. Standard potentials for these waves and rate constants for the decomposition of the 5+ and 6+ species are estimated. The order of stabilities of the highly oxidized forms is Fe(5+) ~ Ru(5+) > Os(6+) > Ru(6+) > Fe(6+).

Introduction

To generate highly oxidizing species electrochemically and to study their properties requires a solvent/supporting electrolyte system that will not oxidize at an electrode until very positive potentials and will not react rapidly with the electrogenerated species. Thus the introduction of acetonitrile and other aprotic solvents allowed the study of radical cations and difficultly oxidized organic and inorganic species. Liquid SO_2 has been especially useful in such studies,[1-8] and by careful purification and the use of tetra-*n*-butylammonium fluoroborate [(TBA)BF_4] as supporting electrolyte, an anodic range to +4 V vs SCE was reported. Previous studies from this laboratory described the electrochemical oxidation of the complexes M(bpy)$_3^{2+}$ (where M = Ru, Fe, and Os and bpy is 2,2′-bipyridine),[1] in SO_2 solutions containing (TBA)BF_4 or (TBA)PF_6 as supporting electrolytes. In these studies, oxidations of the Ru complex to the 4+ form near the oxidation background limit was observed. For the Fe complex, oxidation to both the 4+ and 5+ states was reported. Although reversibility of the $FeL_3^{3+/4+}$ (L = bpy) couple was found with cyclic voltammetry (CV) higher scan rates (≥10 V/s), reactions of the FeL_3^{5+} and the RuL_3^{4+} with a solution component to regenerate the lower oxidized form (in a catalytic reaction mechanism) occurred and reversal (reduction) waves for these species were not seen. With OsL_3^{2+} as starting material, both the 3+ and the 4+ species were stable; more highly oxidized species were not found.

We describe here studies with liquid SO_2 prepared by an improved purification procedure and with (TBA)AsF_6 as supporting electrolyte to produce a significantly extended anodic solvent/electrolyte limit. Moreover, by using an ultramicroelectrode,[9-17]

(1) (a) Gaudiello, J. G.; Sharp, P. R.; Bard, A. J. *J. Am. Chem. Soc.* **1982**, *104*, 6373. (b) Gaudiello, J. G.; Bradley, P. G.; Norton, K. A.; Woodruff, W. H.; Bard, A. J. *Inorg. Chem.* **1984**, *23*, 3.
(2) Tinker, L. A.; Bard, A. J. *J. Am. Chem. Soc.* **1979**, *101*, 2316.
(3) Tinker, L. A.; Bard, A. J. *J. Electroanal. Chem. Interfacial Electrochem.* **1982**, *133*, 275.
(4) Sharp, P. R.; Bard, A. J. *Inorg. Chem.* **1983**, *22*, 2689.
(5) Sharp, P. R.; Bard, A. J. *Inorg. Chem.* **1983**, *22*, 3462.
(6) Anson, F. C.; Collins, J. T.; Gipson, S. L.; Keech, J. T.; Kraft, T. E. *Inorg. Chem.* **1982**, *26*, 1157.
(7) Miller, L. L.; Mayeda, E. A. *J. Am. Chem. Soc.* **1970**, *92*, 5818.
(8) Diethrich, M.; Mortensen, J.; Heinze, J. *Angew. Chem., Int. Ed. Engl.* **1985**, *24*, 508 and references therein.
(9) (a) Wightman, R. M. In *Electroanalytical Chemistry*; Bard, A. J., Ed.; Marcel Dekker: New York, 1988; Vol. 15, in press. (b) Fleishmann, M.; Pons, S.; Rolison, D.; Schmidt, P. P. *Ultramicroelectrodes*; Datatech Science: Morganton, NC, 1987.
(10) Howell, J. O.; Wightman, R. M. *Anal. Chem.* **1984**, *56*, 524.
(11) Howell, J. O.; Wightman, R. M. *J. Phys. Chem.* **1984**, *88*, 3915.

0020-1669/88/1327-4377$01.50/0

we could employ scan rates orders of magnitude larger than in previous studies with larger electrodes so that more highly oxidized forms of the couples could be investigated.

Experimental Section

Apparatus. Electrochemical measurements were made with a home-built bipotentiostat[12] with high sensitivity (20 nA/V) and fast time response capabilities (100 kHz). A PAR Model 175 universal programmer (Princeton Applied Research Corp., Princeton, NJ) was used to control the electrode potential. All current–potential curves were obtained with a Norland digital oscilloscope, Model 3001 (Norland Corp., Fort Atkinson, WI) with a minimum acquisition time of 100 ns/point.

Chemicals. Tetra-*n*-butylammonium hexafluoroarsenate, $(TBA)AsF_6$, was prepared from an aqueous solution of tetra-*n*-butylammonium bromide, (TBA)Br (Southwestern Analytical Chemicals, Austin, TX), to which an equivalent amount of aqueous lithium hexafluoroarsenate (Ozark-Mahoning, Pennwalt Corp., Tulsa, OK) was added. The resulting $(TBA)AsF_6$ crystals were filtered at 0 °C and redissolved in a minimum amount of hot ethyl acetate, to which 10% (v/v) diethyl ether was added. The recrystallization was repeated twice and the isolated product was dried under vacuum at 120 °C for 72 h (mp 245–246 °C). 2,2′-Bipyridyl (Aldrich Chemical Co.), osmium(III) chloride, tris(2,2′-bipyridyl)ruthenium(II) chloride (Alfa Products/Thiokol), and ferrous sulfate (Fisher Scientific) were used as received.

$[Fe(bpy)_3](AsF_6)_2$. Three equivalents of bpy were added to an aqueous solution of $FeSO_4 \cdot 7H_2O$. To the resulting red solution was added an aqueous solution of $LiAsF_6$ to precipitate the AsF_6^- salt. The precipitate was then thrice recrystallized from acetone/ether and dried under vacuum at 80 °C for 24 h.

$[Ru(bpy)_3](AsF_6)_2$. $Ru(bpy)_3Cl_2$ was dissolved in acetone to which 10 equiv of $LiAsF_6$ were added. The $[Ru(bpy)_3](AsF_6)_2$ salt was precipitated by addition of water and filtered. The crystals so obtained were redissolved in acetone to which 5 equiv of $LiAsF_6$ were added. 1% (v/v) ethyl ether was added to this solution and cooled to −20 °C. The recovered material was then recrystallized from acetone/ether and vacuum-dried at 40 °C for 24 h.

$[Os(bpy)_3](AsF_6)_2$. $OsCl_3$ and 3.5 equiv of bpy were added to 50 mL of ethylene glycol and refluxed under dry nitrogen for 72 h. A 50-mL portion of aqueous $LiAsF_6$ containing 5 equiv of AsF_6^- was added to precipitate the corresponding salt. The product was thrice recrystallized from acetone/ether and dried under vacuum at 40 °C for 24 h.

Procedure. Before each experiment a sufficient amount of supporting electrolyte was added to the cell to yield a concentration of 0.1 M. All electrochemical experiments were done in a single compartment cell, fitted with three working electrodes, one counter electrode, and a reference electrode. All potentials are reported versus a silver quasi-reference electrode (AgQRE), which was prepared by dipping an Ag wire in 1 M HNO_3, rinsing with water and acetone, and drying at 70 °C. Potentials given below are referenced to the saturated calomel electrode by measuring the AgQRE potential with respect to the 9,10-diphenylanthracene (DPA)/DPA^+ couple. The compound to be studied was weighed and placed in the sample container. The cell was placed on the vacuum line and heated with a silicone oil bath to 120 °C, while under vacuum (typically (2–6) × 10^{-6} Torr), for at least 24 h. Anhydrous SO_2 gas (Matheson Gas Products, Inc., Houston, TX) (99.99%) was purified by washing with concentrated sulfuric acid and percolated through a P_2O_5 and then a Woelm B-super 1 Alumina (Woelm Phara) column packed on glass wool. SO_2 was condensed into the cell at −70 °C (2-propanol/dry ice bath).

The working electrodes were of Pt wire, 0.5 mm long and 25 μm in diameter, sealed in Pyrex glass tubing. The ultramicroelectrode[9-11] was prepared from 25-μm Pt wire (Alfa Products/Thiokol) that was washed with 30% nitric acid and dried overnight and then placed in a 10 cm long and 1 mm in inner diameter Pyrex tube sealed at one end. The open-ended tube was connected to a vacuum line and heated with a helix heating coil for 1 h, so that any impurities on the Pt surface were desorbed. After high-temperature vacuum cleaning, the wire was sealed by increasing the heating coil temperature. The sealed end of the electrode was polished with sand paper until the wire cross section was exposed and then successively polished with 6-, 1-, and 0.25-μm diamond paste (Buehler Ltd, Lake Bluff, IL). Electrical connection to the Pt wire was made with silver paint to a copper wire. All CV waves were corrected for the solvent background and charging current, and for later waves, the currents were measured from the estimated decaying faradaic current of the preceding wave by following the usual practice.[12a] Controlled-potential coulometry was carried out in a three-compartment cell separated with medium-porosity glass frits. The quasi-reference electrode was placed in the working compartment and separated from it by a fine-porosity glass frit. The working electrode was a 2.5 × 4 cm Pt gauze and the counter electrode was a 1 cm^3 piece of reticular vitreous carbon. The solution was continuously stirred magnetically with a Teflon-coated stirring bar, and the cell was thermostated at −45 °C with a FTS systems cryostat while submerged in an 2-propanol bath.

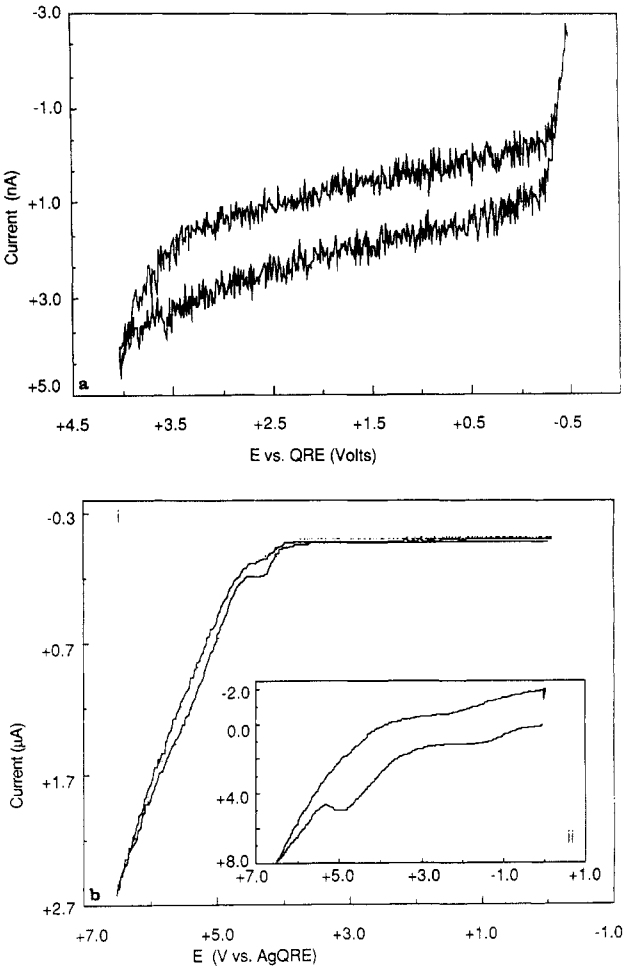

Figure 1. Cyclic voltammogram in liquid SO_2 (at −70 °C) at a 25-μm Pt electrode: (a) 0.1 M $(TBA)AsF_6$, scan rate = 1 V/s; (b) 10 mM $(TBA)AsF_6$, scan rate = 0.5 (i), 2 kV/s (ii).

Results

Background Processes. A typical cyclic voltammogram of background current in liquid SO_2–0.1 M $(TBA)AsF_6$ at −70 °C for a 0.5 mm Pt disk electrode is shown in Figure 1a. The cathodic solvent limit occurred at −0.7 V (current density of 0.2 mA/cm^2). The electrochemical reaction responsible for this solvent limit is attributed to

$$SO_2 + e^- \rightleftharpoons SO_2^{\bullet -} \quad (1)$$

Electron spin resonance (ESR) studies of electroreduced liquid SO_2 solutions after 0.1 and 10 C were passed at −1.0 V vs AgQRE, yielded single lines with g values of 2.048 and 2.053 ± 0.001, respectively. Electrochemically generated $SO_2^{\bullet -}$ in nonaqueous solutions has been reported to dimerize to form $S_2O_4^{2-}$[13a] and to form a charge-transfer complex with SO_2 ($SO_2^{\bullet -}(SO_2)$).[13b] A dependence of the g value with concentration of $SO_2^{\bullet -}$ has been previously reported[13a] and reflects the competing equilibria between

(12) Bard, A. J.; Faulkner, L. R. *Electrochemical Methods*; Wiley: New York, 1980; Chapter 6, p 219, Chapter 11, p 455, and Chapter 13, p 567.
(13) (a) Bonnaterre, R.; Cauquis, G. *J. Electroanal. Chem. Interfacial Electrochem.* **1971**, *32*, 215. (b) Gardner, C. L.; Fouchard, D. T. *J. Phys. Chem.* **1982**, *86*, 3130. (c) Kastening, B.; Gostiša-Mihelčič, B. *J. Electroanal. Chem. Interfacial Electrochem.* **1979**, *100*, 801.
(14) Bauer, D.; Breant, M. In *Electroanalytical Chemistry*; Bard, A. J., Ed.; Marcel Dekker: New York, 1975; Vol. 8, p 300.
(15) Malmsten, R. A.; White, H. S. *J. Electrochem. Soc.* **1986**, *133*, 1067.
(16) Oxidation of TBA^+ ion; details about this reaction will be presented elsewhere: Garcia, E.; Bard, A. J., in preparation.
(17) Nicholson, R. S.; Shain, I. *Anal. Chem.* **1964**, *36*, 706.

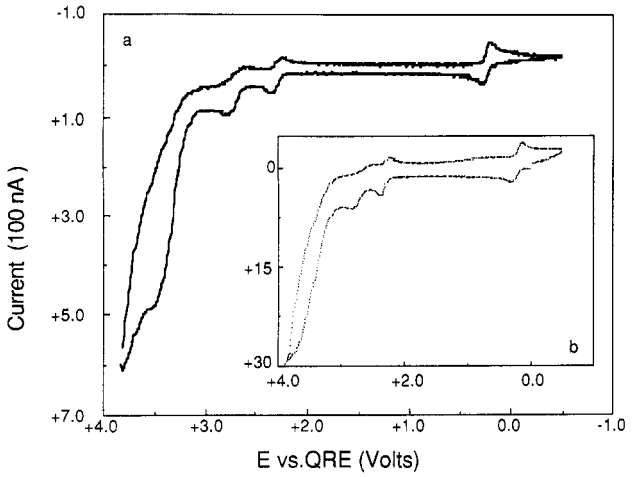

Figure 2. Cyclic voltammogram of 12 mM $[Fe(bpy)_3(AsF_6)_2]$ in liquid SO_2–0.1 M (TBA)AsF_6 at −70 °C at a 25-μm Pt electrode: (a) at 10 V/s; (b) at 100 V/s.

dimerization and charge-transfer complex formation. An ESR spectrum with a g value of 2.044 ± 0.001 was obtained from a saturated $Na_2S_2O_4$ solution in liquid SO_2, which we attribute to $SO_2^{\bullet-}$ formed by the dissociation of $S_2O_4^{2-}$.

The anodic solvent limit with 0.1 M (TBA)AsF_6 occurred at about +4.0 V vs AgQRE (current density of 1 mA/cm^2). This potential is equivalent to about +4.7 V vs SCE; this comparison to the SCE was obtained by calibrating the AgQRE vs the DPA/DPA$^{\bullet-}$ couple and assuming that the half-wave potential for DPA oxidation is solvent independent.[14] This represents a 700-mV increase over the anodic solvent limit previously reported with (TBA)BF_4.[2] If the solvent was purified with the acidic or neutral Woelm alumina previously used instead of the basic (-B) form used in these studies, the background anodic limit was +3.65 V vs AgQRE. Therefore, there would appear to be oxidizable acidic impurities generated in the purification or existing in the solvent. We demonstrated that the limiting anodic electrochemical reaction was oxidation of supporting electrolyte rather than SO_2 by CV studies in a 10 mM solution of (TBA)AsF_6 in SO_2 at an ultramicroelectrode (UME) (Figure 1b). Previous work has demonstrated the advantages of an UME in resistive solutions with low supporting electrolyte concentrations[9-11] and in studies of background processes.[15] The use of a 25-μm Pt UME in this study allowed the acquisition of data for scan rates of 0.2 V/s to 10 kV/s. At this low (TBA)AsF_6 concentration, a single scan-rate-dependent anodic wave was observed at 4.28 V (at 500 mV/s) and at 4.98 V (at 5 kV/s) vs AgQRE, followed by the solvent oxidation about 0.3 V later. The peak current (2 μA at 2 kV/s) was about the same as that expected for a one-electron oxidation of a species at a 10 mM concentration ($D = 10^{-5}$ cm^2/s) at this electrode. A cathodic wave was not observed upon reversal at potentials at the anodic limit for electrolyte oxidation. Because of the absence of a reverse wave, the oxidized electrolyte species is presumed to decompose rapidly after the electron transfer. The dependence of the peak potential (E_{pa}) on scan rate observed for this anodic wave is largely due to the large uncompensated solution resistance (~ 1 M Ω) present in the 10 mM (TBA)AsF_6 solution. An analysis of the behavior of this system is complicated by the fact that the electroactive species is the only electrolyte. A quantitative derivation or simulation of the CV current with this type of system, which must include migrational and diffusional effects, has not yet been reported. Upon addition of more (TBA)AsF_6, the anodic peak height increased linearly with concentration, clearly indicating that the solvent limit noted in this system at usual (TBA)AsF_6 concentrations and at larger electrodes is due to the oxidation of the electrolyte[16] and not the SO_2. Oxidation of SO_2 occurs at potentials beyond +5.0 V and is thus not the limiting process as was previously assumed.[1]

$[Fe(bpy)_3](AsF_6)_2$. Typical cyclic voltammograms for the oxidation of 12 mM $Fe(bpy)_3^{2+}$ at a 25-μm Pt electrode in liquid SO_2 at −70 °C are shown in Figure 2. The formal potentials,

Table I. Formal Potentials for $M(bpy)_3^{n+}$ Complexes

A. Estimated in Liquid SO_2[a]

complex	$E^{\circ\prime}$ in SO_2,[b] V vs SCE	ΔE°_{lim},[c] mV
$[Fe(bpy)_3]^{2+/3+}$	0.87	44
$[Fe(bpy)_3]^{3+/4+}$	2.94	64
$[Fe(bpy)_3]^{4+/5+}$	3.34	129
$[Fe(bpy)_3]^{5+/6+}$	4.3[d]	
$[Ru(bpy)_3]^{2+/3+}$	1.32	37
$[Re(bpy)_3]^{3+/4+}$	3.28	41
$[Ru(bpy)_3]^{4+/5+}$	3.53	156
$[Ru(bpy)_3]^{5+/6+}$	4.5[d]	
$[Os(bpy)_3]^{2+/3+}$	0.91	43
$[Os(bpy)_3]^{3+/4+}$	2.49	58
$[Os(bpy)_3]^{4+/5+}$	3.58	52
$[Os(bpy)_3]^{5+/6+}$	4.1[d]	

B. Literature Values

complex	$E^{\circ\prime}$, V vs SCE	complex	$E^{\circ\prime}$, V vs SCE
$[Fe(bpy)_3]^{3+/2+}$	0.82[e]	$[Os(bpy)_3]^{3+/2+}$	0.82[g]
$[Ru(bpy)_3]^{3+/2+}$	1.354[f]	$[Os(bpy)_3]^{2+/1+}$	−1.26[g]
$[Ru(bpy)_3]^{2+/1+}$	−1.332[f]	$[Os(bpy)_3]^{1+/0}$	−1.45[g]
$[Ru(bpy)_3]^{1+/0}$	−1.517[f]	$[Os(bpy)_3]^{0/1-}$	−1.76[g]
$[Ru(bpy)_3]^{0/1-}$	−1.764[f]		

[a] In 0.1 M (TBA)AsF_6 at −70 °C at a 25-μm Pt electrode. [b] Reference to 9,10-diphenylanthracene, whose oxidation to the radical cation is taken to be solvent independent.[14] [c] See Figure 3 and text. [d] Estimated from the anodic peak potential with some correction for the effect of the following reaction. [e] From ref 21, in MeCN. [f] From ref 18, in MeCN. [g] From ref 22, in H_2SO_4.

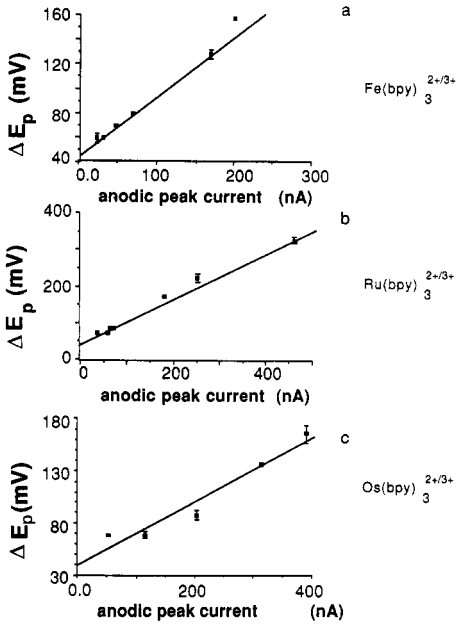

Figure 3. Peak potential difference (ΔE_p) vs anodic peak currents for various scan rates at a 25-μm Pt electrode and −70 °C in SO_2–0.1 M (TBA)AsF_6: (a) for 12 mM $Fe(bpy)_3^{2+/3+}$ (intercept = 43.5 mV); (b) for 8 mM $Ru(bpy)_6^{2+/3+}$ (intercept = 37.5 mV); (c) for 10 mM $Os(bpy)_3^{2+/3+}$ (intercept = 39.6 mV).

$E^{\circ\prime}$, of all waves listed in Table I were estimated from the average values of the peak anodic (E_{pa}) and reverse cathodic (E_{pc}) potentials for scan rates (v) between 2 and 50 V/s.

$$E^{\circ\prime} \cong [(E_{pa} - E_{pc})/2] + E_{pc} \quad (2)$$

The values for the limiting peak splitting (ΔE_{lim}) were obtained from the intercept of a plot of the measured peak splitting ($\Delta E_p = |E_{pa} - E_{pc}|$) versus anodic peak current (i_{pa}) for scan rates between 1 and 500 V/s. This procedure, to a first approximation, compensates for the effect of solution resistance, which is ~0.1 M Ω. Typical plots of ΔE_p are shown in Figure 3, where the

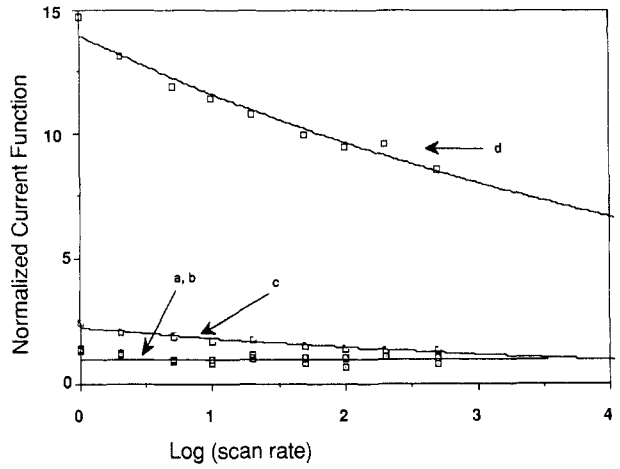

Figure 4. Normalized current function (anodic peak current divided by the square root of scan rate referenced to first wave) as a function of scan rate for a 12 mM $[Fe(bpy)_3(AsF_6)]$ solution in liquid SO_2–0.1 M $(TBA)AsF_6$ at −70 °C at a 25-μm Pt electrode: (a) first wave; (b) second wave; (c) third wave; (d) fourth wave.

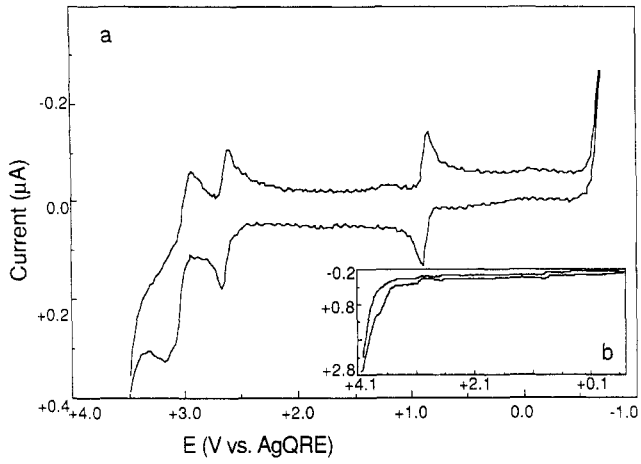

Figure 5. Cyclic voltammogram of 8.0 mM $[Ru(bpy)_3(AsF_6)_2]$ in liquid SO_2–0.1 M $(TBA)AsF_6$ at −70 °C at a 25-μm Pt electrode. Scan rate: (a) 20 V/s; (b) 10 V/s.

intercepts, calculated by a least-squares fitting, are within ±8% of the expected peak splitting of 40 mV for a one-electron reversible couple at −70 °C for $M(bpy)_3^{2+/3+}$.

The first two waves observed for $Fe(bpy)_3^{2+}$ correspond, as previously reported,[1] to two successive nernstian one-electron oxidations to produce the 3+ and 4+ species:

$$Fe^{II}(bpy)_3^{2+} \rightleftharpoons Fe^{III}(bpy)_3^{3+} + e^- \quad E_{pa} = 0.92 \text{ V vs SCE} \quad (3)$$

$$Fe^{III}(bpy)_3^{3+} \rightleftharpoons Fe^{III}(bpy)_2(bpy^{\bullet+})^{4+} + e^- \quad E_{pa} = 3.00 \text{ V vs SCE} \quad (4)$$

For both of these waves the ratio of cathodic to anodic peak currents was essentially one. The first oxidation is known to be a metal-centered one, involving the 2+ and 3+ states.[1] The second wave, at 3.00 V, is thought to be a ligand-centered oxidation that generates the metal-complexed cation radical of the bipyridyl ligand.[1b]

Controlled-potential bulk electrolysis was also employed to demonstrate the reaction stoichiometry and probe the longer term product stability. A 7 mM solution of $Fe(bpy)_3(AsF_6)_2$ was prepared by dissolving 0.253 g of the solid in 40 mL of a 0.1 M $(TBA)AsF_6/SO_2$ solution. When a constant potential of 0.5 V vs AgQRE was applied, the anodic current decayed from its initial value of 2.53 mA to a background level of 36 μA. The total number of coulombs passed was 26.43 C (vs 27.02 C expected for a one-electron reaction). Thus, n_{app} is essentially 1. Similarly, when a potential of 2.45 V vs AgQRE was applied for about 6.5 h, the current decayed to background levels and the total number of coulombs obtained was 25.07 C, yielding $n_{app} = 0.96$. The small difference between these n_{app} values and 1.00 can be attributed to some loss of material from the working compartment by diffusion into the middle and counter electrode compartments, where it precipitates, probably as the red solid, $FeL_3S_2O_4$.

A third wave, at 2.7 V (Figure 2), has an i_{pa} that was larger than the one electron-oxidations typified by the first two waves. A comparison of the $i_{pa}/v^{1/2}$ (currents normalized to $i_{pa}(2+/3+)$) values for all waves as a function of v is shown in Figure 4. As expected, the first two reversible one-electron oxidations show constant values of $i_{pa}/v^{1/2}$.[12b] However, for the third wave, $i_{pa}/v^{1/2}$ decreases with increasing v converging to a one-electron oxidation only at scan rates above 500 V/s. Thus we can assign this wave to a one-electron oxidation perturbed by a following catalytic reaction (an EC′ reaction sequence),[12c] which probably involves the solvent:

$$Fe^{III}(bpy)_2(bpy^{\bullet+})^{4+} \rightleftharpoons Fe^{III}(bpy)(bpy^{\bullet+})_2^{5+} + e^- \quad E_{pa} = 3.44 \text{ V vs SCE} \quad (5)$$

$$Fe^{III}(bpy)(bpy^{\bullet+})_2^{5+} + S \xrightarrow{k_1} Fe^{III}(bpy)_2(bpy^{\bullet+})^{4+} + \text{products} \quad (6)$$

S is the solvent and k_1 is the rate constant for the homogeneous following chemical reaction. We suggest the solvent as the reactant, since no significant change in anodic peak current was observed when different electrolyte concentrations (5, 10, 100 mM) were used.

At fast scan rates (>200 V/s) i_{pa}/i_{pc} for the third wave approached unity, as expected for the proposed mechanism, where the 5+ species can be detected when the characteristic CV time $[\sim(RT/F)/v]$, 85 μs, becomes on the order of the lifetime of the species. Note that in earlier studies[1] a catalytic mechanism was proposed for the 3+/4+ wave, but no analysis of the 4+/5+ wave was possible, mainly because it was close to the background oxidation but also because the high scan rates were not accessible with the large electrode employed in that study. On the basis of extensions of considerations of the 4+ species, the 5+ species can be considered as a +3 iron center coordinated to two bipyridyl radical cations, i.e. $Fe^{III}(bpy)(bpy^{\bullet+})_2^{5+}$.

In this solvent/supporting electrolyte system a fourth oxidation wave, at 3.5 V, is observed (Figure 2), presumably the oxidation of the 5+ to a 6+ species. The i_{pa} value for this wave, which is close to the background oxidation, is larger than those of all of the previous waves. Although the $i_{pa}/v^{1/2}$ value for this wave decreased with increasing v (Figure 4), it did not converge to the value of the other waves at the highest accessible scan rates. The rate of decrease of $i_{pa}/v^{1/2}$ with v was much smaller than that for a simple EC′ mechanism.[12c,17] This would indicate the possibility of other reactions that compete with the primary EC′ reaction or incomplete correction for the background current. No reverse wave was observed for the 6+ species at 500 V/s.

$[Ru(bpy)_3](AsF_6)_2$. Typical cyclic voltammograms for the oxidation of 8 mM $Ru(bpy)_3^{2+}$ at a 25-μm Pt electrode in liquid SO_2 at −70 °C are shown in Figure 5. The cyclic voltammetry is analogous to that of $Fe(bpy)_3^{2+}$. As shown previously, the first two oxidations correspond to successive nernstian one-electron oxidations to produce the 3+ and 4+ species:

$$Ru^{II}(bpy)_3^{2+} \rightleftharpoons Ru^{III}(bpy)_3^{3+} + e^- \quad E_{pa} = 1.35 \text{ V vs SCE} \quad (7)$$

$$Ru^{III}(bpy)_3^{3+} \rightleftharpoons Ru^{III}(bpy)_2(bpy^{\bullet+})^{4+} + e^- \quad E_{pa} = 3.32 \text{ V vs SCE} \quad (8)$$

Again, the ratio of anodic to cathodic peak currents was found to be about one. The third oxidation wave had an i_{pa} value larger than that of the earlier waves at $v = 20$ V/s (Figure 5a). At this v, the ratio of cathodic to anodic peak current is <1. As with the Fe complex, a plot of $i_{pa}/v^{1/2}$ vs v for this wave levels off at fast scan rates (~1 kV/s) to the same value of $i_{pa}/v^{1/2}$ as that for the first two waves (Figure 6). A catalytic mechanism also appears to apply for this wave, i.e.

$$Ru^{III}(bpy)_2(bpy^{\bullet+})^{4+} \rightleftharpoons Ru^{III}(bpy)(bpy^{\bullet+})_2^{5+} + e^- \quad E_{pa} = 3.67 \text{ V vs SCE} \quad (9)$$

$$Ru^{III}(bpy)(bpy^{\bullet+})_2^{5+} + S \xrightarrow{k_1} Ru^{III}(bpy)_2(bpy^{\bullet+})^{4+} + \text{products} \quad (10)$$

Bulk electrolysis was also carried out with this system. A 12 mM solution of $Ru(bpy)_3(AsF_6)_2$ was prepared by dissolving 0.455 g of the solid in 40 mL of a 0.1 M $(TBA)AsF_6/SO_2$ solution. After the current decayed to background values, 46 C had passed, compared to 46.31 C expected for $n_{app} = 1$. Similarly, when a constant potential of 2.75 V vs AgQRE was applied, after 7 h, 45.79 C had passed, yielding $n_{app} = 0.99$ for production of the 4+ species from the 3+ form. This finding demonstrates the long-term stability of the 4+ species, which could be isolated as a green solid. Experiments with this new powerful oxidant are anticipated.

A fourth oxidation wave at 3.7 V vs AgQRE (10 V/s) was also seen in this system (Figure 5b), which showed no cathodic reversal wave at scan rates up to 10 kV/s. This wave has a i_{pa} about 10 times larger than that of a one-electron wave at 10 V/s. A shift in anodic peak potential of 180 mV was observed when the scan rate increased from 1 to 10 V/s. The $i_{pa}/v^{1/2}$ characteristics for this fourth wave are also shown in Figure 6. A rapid decrease of $i_{pa}/v^{1/2}$ with an increase in v was observed. As for the fourth wave observed in the Fe system, the $i_{pa}/v^{1/2}$ vs v behavior does not match theoretical expectations for an EC′ mechanism. This fourth anodic peak current is probably attributable to the oxidation of RuL_3^{5+} to an unstable RuL_3^{6+} species that undergoes reactions which, at least partially, regenerate the 5+ complex. As with the proposed 6+ Fe species, additional complicating reaction pathways or incomplete background current correction is implied.

$$Ru^{III}(bpy)(bpy^{\bullet+})_2^{5+} \rightleftharpoons Ru^{III}(bpy^{\bullet+})_3^{6+} + e^- \quad E_{pa} = 4.4 \text{ V vs SCE} \quad (11)$$

$[Os(bpy)_3](AsF_6)_2$. Typical cyclic voltammograms for the oxidation of 10 mM $Os(bpy)_3^{2+}$ at a 25-μm Pt electrode (in liquid SO_2/0.1 M $(TBA)AsF_6$ at −70 °C), between +1.0 and +3.1 V, are shown in Figure 7a. The first two waves observed, for $[Os(bpy)_3](AsF_6)_3$, correspond to successive nernstian one-electron processes that produce the 3+ and 4+ species:

$$Os^{II}(bpy)_3^{2+} \rightleftharpoons Os^{III}(bpy)_3^{3+} + e^- \quad E_{pa} = 0.90 \text{ V vs SCE} \quad (12)$$

$$Os^{III}(bpy)_3^{3+} \rightleftharpoons Os^{III}(bpy)_3^{4+} + e^- \quad E_{pa} = 2.54 \text{ V vs SCE} \quad (13)$$

The ratio of anodic to cathodic peak currents was about one. The third wave, $E_{pa} = 3.61$ V vs SCE, had an anodic peak height that was about the same as the first two waves, which we assigned to the half-reaction

$$Os^{IV}(bpy)_3^{4+} \rightleftharpoons Os^{IV}(bpy)_2(bpy^{\bullet+})^{5+} + e^- \quad E_{pa} = 3.61 \text{ V vs SCE} \quad (14)$$

This third oxidation appears right at the foot of a larger oxidation wave, as seen in Figure 7b, and the corresponding cathodic wave observed was somewhat smaller than that of the third anodic wave. In previous studies[1] this wave was less apparent and no cathodic wave was observed.

Controlled-potential electrolysis of the $OsL_3^{4+/5+}$ showed evidence of instability of the 5+ form. The current did not decay to background levels and the number of coulombs consumed when i was half of the initial value was about 3 times that expected for $n_{app} = 1$. Presumably, because of the small separation between this process and the 5+/6+ oxidation, the 4+ species is regenerated on this time scale, leading to higher bulk electrolysis currents and large n_{app} values.

The fourth anodic peak observed, Figure 7b, had a peak current about 10 times (at 500 mV/s) and 5 times (at 10 V/s) larger than that of a one-electron wave. A plot of $i_{pa}/v^{1/2}$ vs v is shown in Figure 8. For the first three oxidations $i_{pa}/v^{1/2}$ was constant.[21]

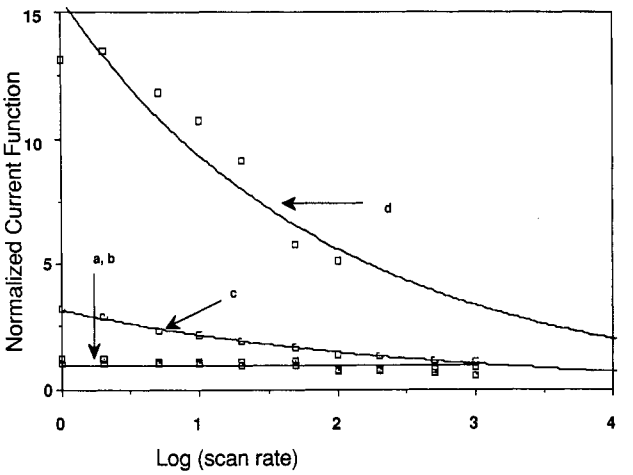

Figure 6. Normalized current function (anodic peak current divided by the square root of scan rate referenced to first wave) as a function of scan rate for a 8.0 mM $[Ru(bpy)_3(AsF_6)_2]$ solution in liquid SO_2–0.1 M $(TBA)AsF_6$ at −70 °C at a 25-μm Pt electrode: (a) first wave; (b) second wave; (c) third wave; (d) fourth wave.

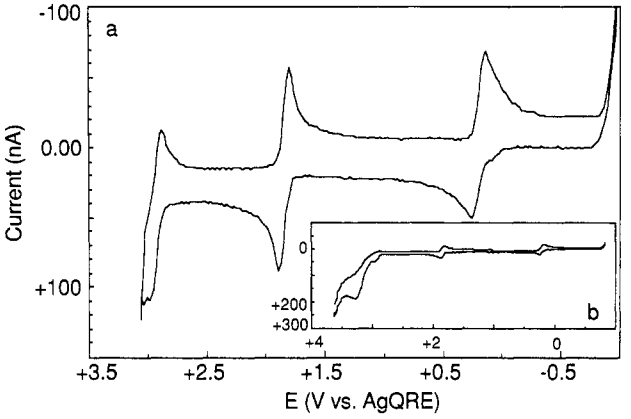

Figure 7. Cyclic voltammogram of 10 mM $[Os(bpy)_3(AsF_6)_2]$ in liquid SO_2–0.1 M $(TBA)AsF_6$ at −70 °C at a 25-μm Pt electrode. Scan rate: (a) 20 V/s, (b) 10 V/s.

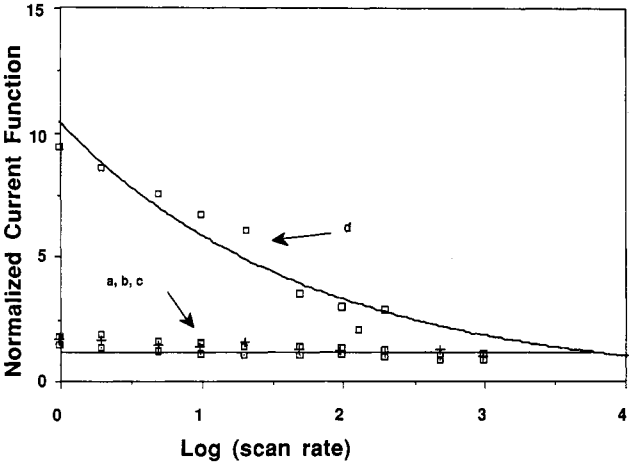

Figure 8. Normalized current function (anodic peak current divided by the square root of scan rate referenced in first wave) as a function of scan rate for a 10 mM $[Os(bpy)_3(AsF_6)_2]$ solution in liquid SO_2–0.1 M $(TBA)AsF_6$ at −70 °C at a 25-μm Pt electrode: (a) first wave; (b) second wave; (c) third wave; (d) fourth wave.

For the fourth wave $i_{pa}/v^{1/2}$ decreased with increasing v, but in contrast with the previous cases, for Fe and Ru 5+/6+, the curve

(18) Tokel-Takvoryan, N. E.; Hemingway, R. E.; Bard, A. J. *J. Am. Chem. Soc.* **1973**, *95*, 6582.
(19) Saji, T.; Aoyagui, S. J. *J. Electroanal. Chem. Interfacial Electrochem.* **1975**, *58*, 401.

approached the one-electron value at large v. However, as with Fe and Ru complexes, the behavior did not match that for an uncomplicated EC′ mechanism.[12c,17] Although no cathodic wave was observed upon reversal at scan rates up to 10 kV/s (due to the proximity to the solvent background process, the faster scan rates were not employed), we feel that this oxidation is best represented by a catalytic oxidation involving the 5+ and 6+ osmium complex and exemplified as

$$Os^{IV}(bpy)_2(bpy^{\bullet+})^{5+} \rightleftharpoons Os^{IV}(bpy)(bpy^{\bullet+})_2^{6+} + e^- \qquad E_{pa} = 4.0 \text{ V vs SCE} \quad (15)$$

$$Os^{IV}(bpy)(bpy^{\bullet+})_2^{6+} + S \xrightarrow{k_1} Os^{IV}(bpy)_2(bpy^{\bullet+})^{5+} + \text{products} \quad (16)$$

Discussion

The observed oxidation of $M^{III}(bpy)_3^{3+}$ (M = Ru, Fe) to the 4+, 5+, and 6+ species in liquid SO_2 is analogous to the reduction of the $Ru^{II}(bpy)_3^{2+}$ species observed in aprotic solvents like MeCN to the +1, 0, and −1 ions.[18,19] These latter species can be described in terms of one, two, or three bpy radical anions coordinated to a Ru(II) center. By analogy, we propose to describe the oxidized species in terms of bpy radical cations coordinated to a M(III) center for M = Ru and Fe and to a M(IV) center for Os.[1] An estimate of the standard potentials for the various half reactions are given in Table I. These values should be good ones for the stable redox pairs (3+/4+) and reasonable approximations for the other couples. While it is true that the CV waves in the latter case are perturbed by the presence of the following reactions consuming product (causing a shift in the wave to potentials less positive that the actual $E°$), this effect tends to be much smaller at an UME because of the high diffusional flux to the small disk.[20] A difference between the bpy reduction series (1+, 0, 1− species) and bpy oxidation series (4+, 5+, 6+) concerns the relative spacing of the waves. The reduction waves are rather closely spaced (Table I), while the oxidation waves are spaced much farther apart. For example, the spacing between the 2+/1+ and 1+/0 waves in MeCN, representing (to a first approximation) additional energy for $Ru(II)(bpy)_2(bpy^{\bullet-})^+$ reduction to $Ru(II)(bpy)(bpy^{\bullet-})_2^0$, is 0.2 V, compared to that for the equivalent oxidation pair, 3+/4+ and 4+/5+ waves, or conversion of $M^{III}(bpy)_2(bpy^{\bullet+})^{4+}$ to $M(III)(bpy)(bpy^+)_2^{5+}$ of ca. 0.4 V in SO_2. This probably reflects the effect of the ionic charge and the relative difficulty of removal of electrons from highly positive centers compared to addition of electrons to positive (or uncharged) ions. The poorer solvating properties of SO_2 compared to MeCN is probably also a factor. Ion pairing of the highly charged species in SO_2 with supporting electrolyte anions undoubtedly occurs to some extent, but the large radii of both $M(bpy)_3^{n+}$ and AsF_6^- will tend to decrease the formation constant of ion pairs compared to those with smaller anions. This trend seems to be followed in the Os species where the spacing between the 4+/5+ and 5+/6+ waves, representing the additional energy to convert $Os^{IV}(bpy)_2(bpy^{\bullet+})^{5+}$ to $Os^{IV}(bpy)(bpy^{\bullet+})_2^{6+}$, is ca. 0.6 V.

While the electrochemical results give clear indication of the instability of the most highly oxidized species and suggest catalytic (EC′) reaction mechanisms, reliable values for the decomposition rate constants cannot be given. The experimental data deviate significantly from the expected theoretical model. This might be due to the presence of unconsidered side reactions, incomplete correction for background current, and, at least at the slower scan rates, an inadequate approximation of the theory for semiinfinite linear diffusion for the EC′ reaction mechanism to the actual situation of hemispherical diffusion (with edge effects) at the UME. However, relative stabilities of the different species can be found.

Conclusions

Studies of the anodic background processes with an UME clearly show that the limiting process in liquid SO_2/0.1 M $(TBA)AsF_6$ is the oxidation of the supporting electrolyte. Thus the available anodic potential range can be extended further by employing a electrolyte more resistive to oxidation.[16] The use of UME's has yielded thermodynamic and kinetic information for the oxidation of $M(bpy)_3^{n+}$ complexes that would be difficult to obtain by other means. Removal of the effect of competing chemical reactions on electron-transfer processes was accomplished by employing very fast scan rates as previously shown for other solvents.[9-11] Clearly, liquid SO_2 is an excellent solvent for electrochemical oxidations. With the added potential range achieved with the new supporting electrolyte [$(TBA)AsF_6$] and the improved purification methods, liquid SO_2 is perhaps the best solvent for the study of highly oxidized species. In this system the 2+, 3+, and 4+ redox states of the Ru and Fe bipyridyl complexes as well as the 3+, 4+, and 5+ Os species are stable on the CV time scale and show reversible waves. The peak potentials of these 3+/4+ redox couples, which are between ca. 2.5 and 3.3 V vs SCE, are among the most positive ones reported for nernstian waves. The 3+ and 4+ Ru, Fe, and Os species can be prepared by bulk electrolysis and are stable for hours. The 4+ Ru and Fe species may thus provide useful new oxidants with very positive redox potentials. The ML_3^{6+} species is produced at the very positive potentials and is unstable and most probably undergoes catalytic reduction with the solvent or electrolyte to regenerate the 5+ complex. This is the first time, to the best of our knowledge, that 5+ and 6+ metal complexes of bipyridyl have been produced in solution. These waves occur at potentials in excess of ca. +4.4 V vs SCE. These highly oxidized species may be useful synthetically for difficult oxidations. Analogous studies of complexes with other ligands, e.g., 1,10-phenanthroline or bipyrazine, should also be of interest. On the basis of the results of this study, we can estimate the relative stability of the highly oxidized species $M(bpy)_3^{n+}$ (order of decreasing stability) as Fe(5+) ~ Ru(5+) > Os(6+) > Ru(6+) > Fe(6+).

Acknowledgment. This work was supported by the National Science Foundation (Grant CHE8402135) and the Welch Foundation (Grant F-079). The assistance of Dr. Angel E. Kaifer in obtaining the ESR spectra is gratefully acknowledged. We also thank Dr. Alan Bond for his suggestions and useful discussions.

Registry No. $[Fe(bpy)_3](AsF_6)_2$, 117251-26-0; $[Ru(bpy)_3](AsF_6)_2$, 117251-27-1; $[Os(bpy)_3](AsF_6)_2$, 117251-28-2; $[Fe(bpy)_3]^{2+}$, 15025-74-8; $[Fe(bpy)_3]^{3+}$, 18661-69-3; $[Fe(bpy)_3]^{4+}$, 83207-86-7; $[Fe(bpy)_3]^{5+}$, 83207-88-9; $[Fe(bpy)_3]^{6+}$, 117251-29-3; $[Ru(bpy)_3]^{2+}$, 15158-62-0; $[Ru(bpy)_3]^{3+}$, 18955-01-6; $[Ru(bpy)_3]^{4+}$, 83207-87-8; $[Ru(bpy)_3]^{5+}$, 117251-30-6; $[Ru(bpy)_3]^{6+}$, 117251-31-7; $[Os(bpy)_3]^{2+}$, 23648-06-8; $[Os(bpy)_3]^{3+}$, 30032-51-0; $[Os(bpy)_3]^{4+}$, 87901-16-4; $[Os(bpy)_3]^{5+}$, 117251-32-8; $[Os(bpy)_3]^{6+}$, 117251-33-9; SO_2, 7446-09-5; Pt, 7440-06-4; $(TBA)AsF_6$, 22505-56-2; $Ru(bpy)_3Cl_2$, 14323-06-9; $LiAsF_6$, 29935-35-1; 2,2′-bipyridine, 366-18-7.

(20) Dayton, M. A.; Brown, J. C.; Stutts, K. J.; Wightman, R. M. *Anal. Chem.* **1980**, *52*, 946.
(21) Abruna, H. D. *J. Electroanal. Chem. Interfacial Electrochem.* **1984**, *175*, 321.
(22) Chen, Y. D.; Santhanam, K. S. V.; Bard, A. J. *J. Electrochem. Soc.* **1981**, *128*, 1460.